Quest Journals Journal of Research in Humanities and Social Science Volume 13 ~ Issue 10 (October 2025) pp: 104-111 ISSN(Online):2321-9467



Research Paper

www.questjournals.org

Characterizing the Structure-based Mechanism Between Aurigene Compound 16 and PD-1 by AutoDock Vina

Yichen He

(The Experimental High School Attached to Beijing Normal University)

ABSTRACT: The Programmed Death Receptor-1/ Programmed Death Ligand-1(PD-1/PD-L1) pathway is a crucial target in cancer immunotherapy, with monoclonal antibodies (MAbs) currently dominating clinical applications. However, the limited efficacy and significant side effects of MAbs highlight the need for alternative therapeutic strategies. In this study, we investigate the structure-based binding mechanism between the immune checkpoint protein PD-1 and Aurigene compound 16, a novel small-molecule inhibitor. Using molecular docking simulations via AutoDock Vina, we demonstrate that Aurigene compound 16 binds to PD-1 with binding affinity -5.7 kcal/mol, and its interactions include 9 hydrogen bonds, 1 hydrophobic interaction, and 2 salt bridges. The small-molecule compound effectively occupies the interface between PD-1 and PD-L1. This interaction suggests that Aurigene compound 16 may serve as a competitive inhibitor. These findings provide insights for PD-1 and PD-L1 targeted small-molecular drug development.

KEYWORDS: Computational Biomodeling, Immune Checkpoint Inhibitors, PD-1, Small Molecular Drugs, Molecular Docking.

Received 04 Oct., 2025; Revised 12 Oct., 2025; Accepted 14 Oct., 2025 © The author(s) 2025. Published with open access at www.questjournas.org

I.INTRODUCTION

In recent years, cancer has gained international recognition as one of the most problematic chronic illnesses. In the major causes of death in the US in 2022, it came in second, trailing only heart attacks. In humans, there is a wide range of possible cancerous appearances. For example, when sorted by its form, cancer can be classified into solid tumors, leukemia, and lymphoma. When categorized by the organism on which it resides, there are numerous varieties, with lung cancer, breast cancer, and cancer of the colon and rectum being the most prevalent examples. The intricacy of the genesis of cancer, combined with its variation among individuals, is severely impeding the progression of cancer research and treatment.

The currently existing treatments for cancer mainly include surgery, radiotherapy, chemotherapy, targeted therapy, and immunotherapy. The first three methods introduce artificially designed pathways targeted directly to kill cancer cells. Conversely, the principle of immunotherapy is to engage the naturally occurring antitumor immune response in the human body. Immunotherapy mainly consists of immune checkpoint inhibitors (ICIs), adoptive cell transfer, oncolytic virus therapy, and therapeutic vaccines.³ Immune checkpoint inhibitor is a fast-developing cancer treatment. They strengthen the anti-tumor effect based on the human body's existing immune responses, identified as the tumor immune cycle (TIC).⁴ The immune escape of tumor cells is one of the biggest weakening factors of the TIC, including the interactions with the immune checkpoint proteins.⁵

The programmed death receptor 1 (PD-1) is an immune checkpoint expressed on immunocytes. The presence of PD-1 on T-cells functions to negatively regulate their activities. Specifically, through the joining of PD-1 with its ligand programmed cell death 1 ligand 1 (PD-L1) or programmed cell death 1 ligand 2 (PD-L2), tumor-specific T-cells are suppressed in T-lymphocyte proliferation, cytokine secretion, and cytotoxic functions, thus leading to exhaustion.⁶ Noticeably, under healthy conditions, the negative modulation of immune reaction caused by the PD-1/PD-L1 pathway is beneficial, as it prevents overstimulation and sustains immunological self-tolerance.⁷ However, in the tumor microenvironment, PD-1 is often found to be overexpressed, leading to an excess of T-cell deficiency and worsening the health condition of individuals afflicted with cancer.⁸ Therefore, blocking the interaction of PD-1 with its ligand or other similar immune checkpoint pathways can prevent tumor-specific T-cells from exhaustion and therapeutically treat cancer.

ICIs are a significant breakthrough in cancer immunotherapy.⁵ By preempting the target spot where inhibitory receptors bind, ICIs restrain the tumor cells from immune escape and promote the immune reaction.⁴ Existing ICIs are agents that function as a competitive blockade of inhibitory receptors, most of which belong to monoclonal antibodies (MAbs).⁵ For instance, antibody agents pembrolizumab and nivolumab are pioneering checkpoint inhibitors aiming at PD-1. In 2014, they were approved by the Food and Drug Administration (FDA), mainly indicating non-small-cell lung cancer (NSCLC)and melanoma; they have shown great clinical performance in prolonging patients 'progression-free survival (PFS).²

In general, immune checkpoint inhibitors of the antibody type show effectiveness, but in limited cancer categories and an insufficient proportion of patients. Additionally, the long half-life and high target engagement of MAbs manifest clinically in immune-related side effects. Differentiating from monoclonal antibodies, small-molecule ICIs better prevent adverse events and hold a higher efficiency resulting from mitigative target occupancy and modulation of drug half-life. Based on these features, they may potentially become alternatives to ICIs in the form of antibodies because they would probably overcome the imperfections of peptide-based inhibitors. The investigation of small-molecule strategies holds broad but challenging prospects.

Although ICIs in the form of antigens have developed sufficiently, only inchoate investigations on small-molecule ICIs have been conducted, probably due to the absence of structural information. Starting in 2011, scientists have disclosed many small-molecule chemical compounds as PD-1/PD-L1 modulators. For example, Harvard scientists disclosed Harvard compounds as the earliest leading basis as small-molecule PD-1 inhibitors, and a set of PD-L1-targeting biphenyl derivatives has been discovered by Bristol-Myers Squibb (BMS). Several of these compounds have high potential to disrupt PD-1/PD-L1 interactions; however, their detailed structure-activity relationships, as well as the efficiency of these compounds on the surface of cancer cells, remain uncertain.

In this study, we investigate the binding mechanism between PD-1 and its small-molecule ligand, commonly referred to as Aurigene compound 16, which is identified in PubChem¹² under the Compound Identifier (CID) 134827773. Notably, a search for "Aurigene compound 16" in PubChem yields two distinct entries, corresponding to CIDs 134827773 and 122541438. Despite differences in their listed synonyms, a comparison of the sub-pages reveals that both entries share the same chemical structure, molecular formula (C₁₄H₂₃N₇O₆), and molecular weight (385.38 g/mol). For our simulation, we utilized the compound file associated with CID 134827773 and consistently refer to it as Aurigene compound 16. This small molecule, a peptidomimetic immunomodulator developed by Aurigene Pharmaceuticals, shows promise as an immune checkpoint inhibitor. However, its precise mechanism of action—whether it disrupts the PD-1/PD-L1 interaction or modulates PD-1 activity—remains to be fully revealed. Further research is essential to unlock the full therapeutic potential of Aurigene compound 16.

Structure-based drug design utilizes the data of macromolecular targets to design or alter the composition of chemical compounds with effective binding affinities.¹³ In a structure-based drug design process, steps are taken to determine potential ligands and optimize their affinity and efficiency, such as multiple times of observing the intermolecular connections, uncovering unidentified binding sites, and conducting a mechanism assessment. Structural information for structure-based analysis is typically acquired from simulation methods or generated via computational techniques such as molecular modeling and molecular docking.¹⁴

Computational methods have been increasingly adopted in drug-designing processes to analyze structural information. Molecular docking is a critical computational technique employed in structure-based drug design, allowing the prediction of the preferred orientation of a ligand when bound to a target protein. It reveals accurate statistics of the position and energy expenditure of the interactions. AutoDock Vina¹⁵ is an application designed to simulate the molecular docking process. It is equipped with a higher speed and accuracy, compared to the previous version of the molecular docking tool.

In this article, we present a holistic report of the simulated molecular docking of PD-1 with the small molecule ligand Aurigene compound 16, operated by AutoDock Vina. Based on the structure and interaction site from the Protein Data Bank (PDB) format of the docking result, we provide explanations and analysis of the binding mechanism, extracting insights into directions of further investigation in the Aurigene compound 16.

II.METHODS

i. Molecular Docking and Visualization

The ligand Aurigene compound 16 was retrieved in Structure-Data File (SDF) format from PubChem. Its CID is 134827773. The target protein structure of human PD-1 was downloaded from the AlphaFold Protein Structure Database^{16 17} in PDB format. Its UniProt ID is Q15116. The PyMOL 3.0¹⁸ software was utilized for several preparatory steps, including the transformation of the SDF file to PDB format, the removal of unnecessary protein tails, and the generation of publication-quality figures.

The ligand was converted from SDF to PDB format using PyMOL. Protein tail regions, which are often disordered and non-essential for docking, were removed using the remove command to simplify the structure and focus the docking analysis on the relevant binding sites. The ray command in PyMOL was used to render high-resolution figures of the docked complexes, highlighting the key interactions.

Pre-treatment of the PD-1 protein and Aurigene compound 16 for docking was conducted using Molecular Graphics Laboratory Tools (MGLTools)¹⁹ 1.5.7, a suite of utilities designed for the preparation of input files for AutoDock Vina. The ligand and protein structure were prepared by adding polar hydrogen atoms and assigning Gasteiger charges to ensure accurate docking simulations. The grid box was defined around the PD-1 active site using MGLTools 'AutoGrid module to focus the docking simulation on the relevant region of the protein.

The docking parameters were optimized to achieve the best possible binding affinity prediction, with the exhaustiveness parameter set to 8 to balance accuracy and computational efficiency. Multiple docking runs were conducted to ensure the reliability of the predicted binding modes.

Post-docking analysis was carried out using the Protein-Ligand Interaction Profiler (PLIP),20 an online tool that provides detailed insights into the interactions between the ligand and protein. PLIP was used to identify and visualize the hydrogen bonds, hydrophobic interactions, and salt bridge interactions between PD-1 and Aurigene compound 16. The results were then visualized and further analyzed using PyMOL to confirm the docking predictions and to prepare the figures for publication

ii. Docking Parameters Optimization

During the docking simulation, the configuration yielding the greatest affinity was chosen to identify the ideal parameter pairing. Table 1 provides further specifics on these parameters.

Table 1. Other parameters in molecular docking were generated. This table records the specific parameters applied in the simulation. The first and second columns show the center coordinate and the size of the grid box, respectively. In the third column, the num_modes was set to 9, meaning that a total of 9 conformations will be generated.

Parameter	Value (Å)	Parameter	Value (Å)	Parameter	Value
center_x	-13.088	size_x	13.5	num_modes	9
center_y	3.74	size_y	26.25	energy_range	3
center_z	1.677	size_z	26.25	сри	4

III.RESULTS

i. Overall Binding Orientation

The overall outcome is given in Figure 1. The docking results reveal that Aurigene compound 16 binds to the external surface of PD-1's mid-structure beta sheets without engaging the adjacent alpha helices. The visualization emphasizes the specific interaction site, suggesting a potential competitive inhibition mechanism by occupying the binding site typically associated with PD-L1.

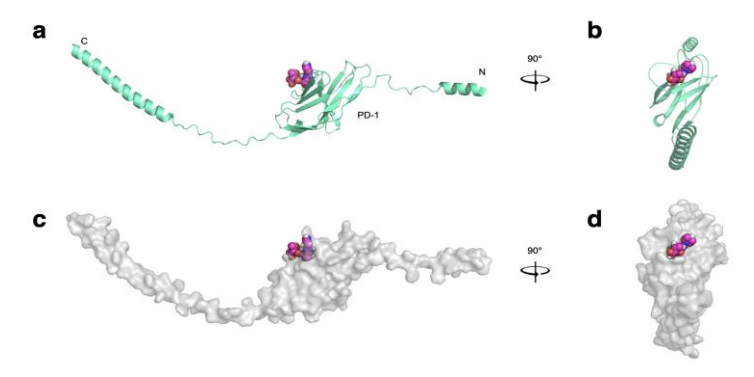


Figure 1. Binding Orientation of Aurigene Compound 16 within the PD-1 Protein Structure. This figure presents a molecular docking analysis illustrating the interaction between Aurigene compound 16 and the PD-1 protein. Figure 1a and Figure 1c offer front views of the docking configuration, while Figure 1c and Figure 1d provide side views rotated 90 degrees to the right.

ii. Molecular Docking Results

AutoDock Vina provides the Affinity and the distance from the best mode of 9 versions of conformation, as shown in Table 2. The Binding affinity measures the binding free energy, reflecting the energy change in the system, in kcal/mol. A more negative value suggests a stronger binding, meaning that more energy is required to dissociate them, and the interaction between the ligand and the protein is more stable. The columns Rmsd l.b. and Rmsd u.b. represent the Lower Bound Root Mean Square Deviation and the Upper Bound Root Mean Square Deviation, respectively. They are different Root Mean Square Deviation (RMSD) calculations that indicate the difference between the predicted docking conformation and the reference structure (Mode 1).

Table 2. Nine versions of molecular Docking conformation. Mode 1 indicates the strongest interaction between the Aurigene compound 16 and PD-1, with the lowest binding affinity of -5.7 kcal/mol. The remaining 8 conformations exhibit weaker affinities. Mode 1 serves as the reference (RMSD=0.000) of the RMSD calculations of the other 8 conformations that have varying RMSD values.

Mode	Affinity	Distance from the best mode						
	(kcal/mol)	Rmsd 1.b.	Rmsd u.b.					
1	-5.7	0.000	0.000					
2	-5.6	1.276	1.398					
3	-5.0	2.392	6.817					
4	-5.0	1.894	2.308					
5	-5.0	13.056	16.184					
6	-4.8	14.715	15.918					
7	-4.8	11.720	13.877					
8	-4.8	11.823	13.443					
9	-4.8	2.683	6.391					

iii. Protein-Ligand Interaction Profile

We applied the PLIP tool to make a detailed assessment of the interactions between PD-1 and Aurigene compound 16. Visualization of the interactions is presented in Figure 2, and specific parameters are shown in Table 3. Among the variety of ways in which a protein interacts with a small molecule, three kinds of protein-ligand interactions can be identified between PD-1 and Aurigene compound 16. They include hydrogen bonds, hydrophobic interactions, and salt bridges. The PLIP detected a significant quantity of nine hydrogen bonds. Therefore, to illustrate the arrangement of all hydrogen bonds in clarity, an additional Figure 2a depicting hydrogen bond interactions from a different visual perspective is added as a supplement to the primary Figure 2b.

A total of three types of interactions are identified between PD-1 and Aurigene compound 16. The first and most significant type of interaction is hydrogen bonds. Five amino acids (aa), including Cysteine-93 (CYS-93), Glutamic acid-84 (GLU-84), Valine-97 (VAL-97), Glutamine-91 (GLN-91), and Alanine-80 (ALA-80), are involved in the nine hydrogen bonds. The atoms participating in hydrogen bonds from the small molecule include Oxygen, Nitrogen, and Hydrogen. The primary structure is considered to be 6 aa. The average interaction distance across these bonds is approximately 3.4 Angstroms. Among the residues that participate in hydrogen bond interactions, the residue GLU-84 is the primary source, providing 4 hydrogen bonds from two different atoms. One hydrophobic interaction is observed between ALA-80's carbon beta and the carbon atom of the ligand. The primary structure of the protein is 1 aa. It is estimated to occur at a distance of 3.7 Angstroms. Two salt bridges regarding two residues are identified: Arginine-90 (ARG-90) and GLU-84. The average distance of these forces is about 4.5 Angstroms.

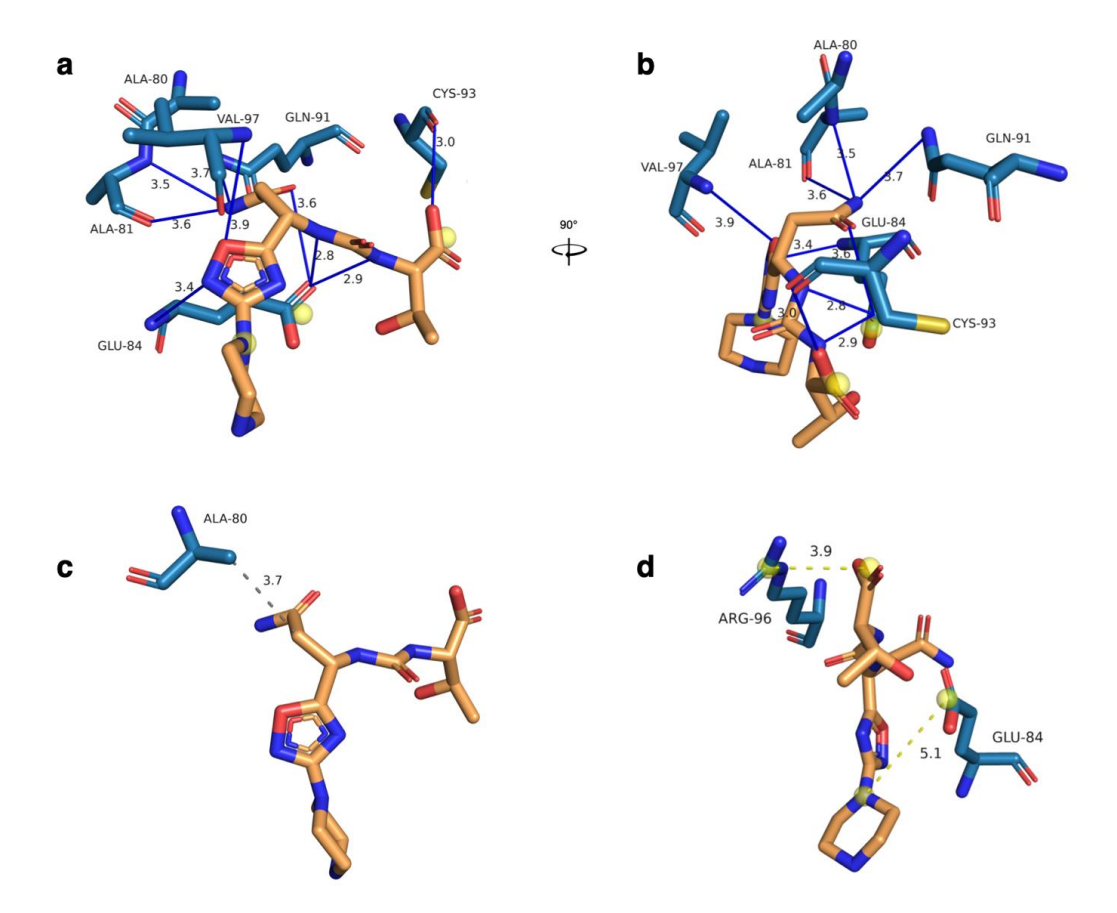


Figure 2. Visualization of binding interactions. In this group of figures, the structure of the ligand Aurigene compound 16 is presented in yellow, and the residues that are involved in the interactions are shown in blue. Figure 2a and Figure 2b depict the hydrogen bonds from two different visual viewpoints. Figure 2c presents the hydrophobic interaction in a grey dotted line, and Figure 2d presents salt bridges. Each "ALA-84"-like character is used to identify the name of the residue next to it. The non-integer numbers indicate the interaction distances.

Table 3. Interaction profile. This table provides a detailed description of each specific interaction between Aurigene compound 16 and PD-1. For each interaction, the specific residue and the amino acid are identified to locate the interaction in the protein, and the bond distances are provided as well. Specifically, there are different additional measures regarding each interaction type to ensure a sufficient evaluation through multiple dimensions.

	Index	Residue	AA	Distance	Ligand Atom	Protein Atom				
Hydrophobic Interactions	1	80A	ALA	3.7	31	753				
	Index	Residue	AA	Distance H-A	Distance D-A	Donor Angle	Protein donor?	Side chain	Donor Atom	Acceptor Atom
	1	81A	ALA	2.51	3.53	173.96	$\sqrt{}$	×	755[Nam]	34[Nam]
	2	81A	ALA	2.58	3.59	171.06	×	×	34[Nam]	758[O2]
	3	84A	GLU	2.31	2.91	116.06	×	$\sqrt{}$	5[Nam]	787[O3]
Hydrogen Bonds	4	84A	GLU	2.19	2.83	119.26	×	$\sqrt{}$	2[Nam]	787[O3]
	5	84A	GLU	2.76	3.61	150.41	$\sqrt{}$	$\sqrt{}$	787[O3]	33[O2]
	6	84A	GLU	3.06	3.40	100.47	$\sqrt{}$	×	780[Nam]	19[Nox]

	7	91A	GLN	3.27	3.73	109.31	\checkmark	$\sqrt{}$	855[Nam]	34[Nam]
	8	93A	CYS	2.68	3.04	101.99	×	×	15[O.co2]	872[O2]
	9	97A	VAL	3.06	3.92	143.12	\checkmark	×	922[Nam]	18[O3]
	Index	Residue	AA	Distance	Protein positive?	Ligand Group	Ligand Atoms			
Salt Bridges	Index	Residue 84A	AA GLU	Distance 5.11		Ligand Group Tertamine	-			

iv. Interference Comparison

A comparison of the binding coordination between Aurigene compound 16 and PD-L1 on PD-1 is presented in Figure 3, highlighting the molecular interactions that each ligand forms within the PD-1 binding pocket. Aurigene compound 16 is located on the green colored end of PD-1, and similarly, PD-L1 is located on the green end as well. The PD-L1's interaction with PD-1 contributes to a complete dimer structure, and thus to the immune-suppressive interaction. However, as Aurigene compound 16 occupies the coordination site PD-L1 would need on PD-1, we hypothesize that Aurigene compound 16 could act as an occupying blockade to inhibit the interference between PD-1 and PD-L1.

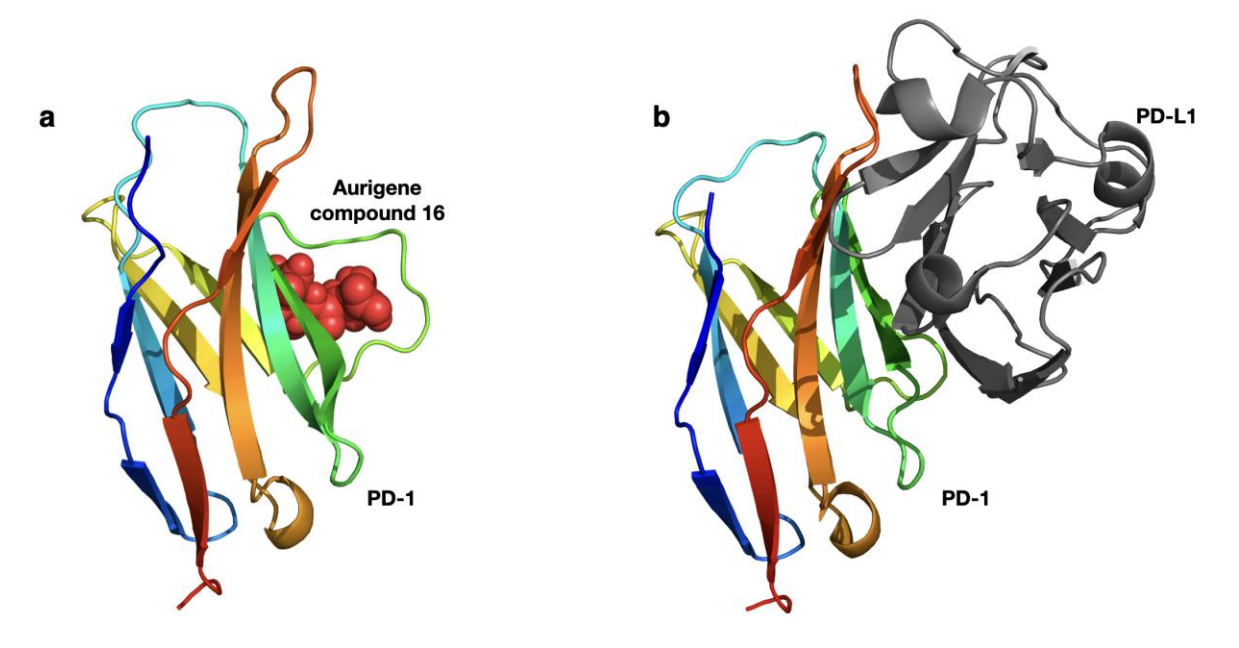


Figure 3. Binding coordination comparison. Figure 3a and Figure 3b depict the complex structure of PD-1 with Aurigene compound 16 and the dimer of PD-1 with PD-L1, respectively. In both Figure 3a and Figure 3b, PD-1 is shown in rainbow-colored ribbons. Aurigene compound 16 is presented in red spheres in Figure 3a, and PD-L1 is shown in grey ribbons in Figure 3b.

Table 3. Interaction profile. This table provides a detailed description of each specific interaction between Aurigene compound 16 and PD-1. For each interaction, the specific residue and the amino acid are identified to locate the interaction in the protein, and the bond distances are provided as well. Specifically, there are different additional measures regarding each interaction type to ensure a sufficient evaluation through multiple dimensions.

	Index	Residue	AA	Distance	Ligand Atom	Protein Atom				
Hydrophobic Interactions	1	80A	ALA	3.7	31	753				
	Index	Residue	AA	Distance H-A	Distance D-A	Donor Angle	Protein donor?	Side chain	Donor Atom	Acceptor Atom
	1	81A	ALA	2.51	3.53	173.96	$\sqrt{}$	×	755[Nam]	34[Nam]
	2	81A	ALA	2.58	3.59	171.06	×	×	34[Nam]	758[O2]
	3	84A	GLU	2.31	2.91	116.06	×	\checkmark	5[Nam]	787[O3]
Hydrogen Bonds	4	84A	GLU	2.19	2.83	119.26	×	$\sqrt{}$	2[Nam]	787[O3]
	5	84A	GLU	2.76	3.61	150.41	$\sqrt{}$	$\sqrt{}$	787[O3]	33[O2]
	6	84A	GLU	3.06	3.40	100.47	$\sqrt{}$	×	780[Nam]	19[Nox]
	7	91A	GLN	3.27	3.73	109.31	$\sqrt{}$	$\sqrt{}$	855[Nam]	34[Nam]
	8	93A	CYS	2.68	3.04	101.99	×	×	15[O.co2]	872[O2]
	9	97A	VAL	3.06	3.92	143.12	$\sqrt{}$	×	922[Nam]	18[O3]
	Index	Residue	AA	Distance	Protein positive?	Ligand Group	Ligand Atoms			
Salt Bridges	1	84A	GLU	5.11	×	Tertamine	24			
	2	96A	ARG	3.88	$\sqrt{}$	Carboxylate	14,15			

IV.DISCUSSION

The PD-1/PD-L1 pathway is a leading field in the development of immune checkpoint inhibitors and cancer immunotherapy. The existing antibody agents that belong to immune checkpoint inhibitors are well-studied, providing researchers with fewer opportunities to achieve further progress. Moreover, there are significant side effects of MAbs. Consequently, the discovery of immune checkpoint inhibitors that are small molecules is highly valuable. Based on the results, it can be concluded that Aurigene compound 16 has the structural potential to become a small-molecule compound as a peptidomimetic immunomodulator aiming at the PD-1/PD-L1 pathway.

The outcome of the simulated docking operated by AutoDock Vina suggests that Aurigene compound 16 successfully binds with PD-1, with an optimal of -5.7 kcal/mol. The analysis of interactions operated by the PLIP identified possibly 9 hydrogen bonds, 1 hydrophobic contact, and 2 π -cation engagements. Noticeably, the number of hydrogen bonds we identified here is surprisingly big. Hydrogen bonds are a powerful source of the binding force of drugs and proteins, and the number of hydrogen bonds indicates the probable efficiency of the small molecule ligand. The number of 9 hydrogen bonds located in the binding interactions between PD-1 and Aurigene compound 16 explains that this small molecule compound is highly effective from a structural perspective.

Differentiating from many small-molecule drugs that bind with the protein in a deep-seated protein pocket, the binding coordination of the Aurigene compound 16 on PD-1 is located at the surface of the protein. According to this statement, the affinity of the Aurigene compound 16 with PD-1 may be poor. However, the PD-1 and PD-L1 compound structure is what decisively influences the activity of T-cells. Therefore, we presume that Aurigene compound 16 effectively inhibits the interaction between PD-1 and PD-L1 by competitively occupying the coordination site on PD-1, which PD-L1 would otherwise possess. A rough comparison of the binding site of Aurigene compound 16 and PD-L1 on PD-1 is conducted, based on the Aurigene compound 16 and PD-1 complex structure obtained from our simulation result and the crystal structure of the PD-1 and PD-L1 dimer downloaded

from the wwPDB database. As depicted in Figure 3, the binding coordination of the Aurigene compound 16 on PD-1 and PD-L1 on PD-1 approximately overlaps. Further observation of the crystal structure supports the thesis that when bound together, the Aurigene compound 16 competitively registers one of the residues on the PD-1 pocket that would be required to be spare to form a dimer structure with PD-L1, and thus effectively blocks the interaction between PD-1 and PD-L1. In conclusion of the above results, the structural analysis supports the assumption that Aurigene compound 16 is a PD-1/PD-L1 pathway inhibitor that functions by directly blocking the interaction of PD-1 and PD-L1 as a competitive inhibitor.

V.CONCLUSION

According to results drawn from this study, from the structural perspective, the usage of Aurigene compound 16 is a sufficiently applicable method to block the PD-1/PD-L1 pathway. The interaction force between Aurigene compound 16 and PD-1 is significantly high, and the binding site can be considered more energy-efficiently. Unlike most of the existing PD-1/PD-L1 pathway inhibitors are either inhibitors only targeting PD-1 or PD-L1 in the form of MAbs whose interaction with PD-1/PD-L1 covers a wide area, Aurigene compound 16, as a small molecule chemical compound, is capable of landing more precisely at an exact small coordination. This capability enables small-molecule drugs like Aurigene compound 16 to inhibit both the proteins PD-1 and PD-L1 by directly occupying their binding coordination.

REFERENCES

- Roy, P.; Saikia, B. Cancer and Cure: A Critical Analysis. Indian Journal of Cancer 2016, 53 (3), 441. DOI:10.4103/0019-509x.200658.
- [2]. Schwartz, S. M. Epidemiology of Cancer. Clinical Chemistry 2024, 70 (1), 140–149. DOI:10.1093/clinchem/hvad202.
- [3]. Jiao, P.; Geng, Q.; Jin, P.; Su, G.; Teng, H.; Dong, J.; Yan, B. Small Molecules as PD-1/PD-L1 Pathway Modulators for Cancer Immunotherapy. *Current Pharmaceutical Design* **2019**, *24* (41), 4911–4920. DOI:10.2174/1381612824666181112114958.
- [4]. Moslehi, J.; Lichtman, A. H.; Sharpe, A. H.; Galluzzi, L.; Kitsis, R. N. Immune Checkpoint Inhibitor–Associated Myocarditis: Manifestations and Mechanisms. *Journal of Clinical Investigation* **2021**, 131 (5). DOI:10.1172/jci145186.
- [5]. Chen, D. S.; Mellman, I. Oncology Meets Immunology: The Cancer-Immunity Cycle. *Immunity* 2013, 39 (1), 1–10. DOI:10.1016/j.immuni.2013.07.012.
- [6]. Wherry, E. J. T. Cell Exhaustion. *Nature Immunology* **2011**, *12* (6), 492–499. DOI:10.1038/ni.2035.
- [7]. Wang, Q.; Bardhan, K.; Boussiotis, V. A.; Patsoukis, N. The PD-1 Interactome. Advanced Biology 2021, 5 (9). DOI:10.1002/adbi.202100758.
- [8]. Zak, K. M.; Grudnik, P.; Magiera, K.; Dömling, A.; Dubin, G.; Holak, T. A. Structural Biology of the Immune Checkpoint Receptor PD-1 and Its Ligands PD-L1/PD-L2. Structure 2017, 25 (8), 1163–1174. DOI:10.1016/j.str.2017.06.011.
- [9]. Naimi, A.; Mohammed, R. N.; Raji, A.; Chupradit, S.; Yumashev, A. V.; Suksatan, W.; Shalaby, M. N.; Thangavelu, L.; Kamrava, S.; Shomali, N.; Sohrabi, A. D.; Adili, A.; Noroozi-Aghideh, A.; Razeghian, E. Tumor Immunotherapies by Immune Checkpoint Inhibitors (Icis): the Pros and Cons. Cell Communication and Signaling 2022, 20 (1). DOI:10.1186/s12964-022-00854-y.
- [10]. Sasikumar, P. G.; Ramachandra, M. Small-Molecule Immune Checkpoint Inhibitors Targeting PD-1/PD-L1 and Other Emerging Checkpoint Pathways. *BioDrugs* **2018**, *32* (5), 481–497. DOI:10.1007/s40259-018-0303-4.
- [11]. Zak, K. M.; Kitel, R.; Przetocka, S.; Golik, P.; Guzik, K.; Musielak, B.; Dömling, A.; Dubin, G.; Holak, T. A. Structure of the Complex of Human Programmed Death 1, PD-1, and Its Ligand PD-L1. Structure 2015, 23 (12), 2341–2348. DOI:10.1016/j.str.2015.09.010.
- [12]. 12. Kim, S.; Chen, J.; Cheng, T.; Gindulyte, A.; He, J.; He, S.; Li, Q.; Shoemaker, B. A.; Thiessen, P. A.; Yu, B.; Zaslavsky, L.; Zhang, J.; Bolton, E. E. PubChem 2023 Update. *Nucleic Acids Research* 2022, 51 (D1). DOI:10.1093/nar/gkac956.
- [13]. Colman, P. M. Structure-Based Drug Design. Current Opinion in Structural Biology 1994, 4 (6), 868–874. DOI:10.1016/0959-440x(94)90268-2.
- [14]. Ferreira, L.; Dos Santos, R.; Oliva, G.; Andricopulo, A. Molecular Docking and Structure-Based Drug Design Strategies. *Molecules* **2015**, 20 (7), 13384–13421. DOI:10.3390/molecules200713384.
- [15]. Trott, O.; Olson, A. J. Autodock Vina: Improving the Speed and Accuracy of Docking with a New Scoring Function, Efficient Optimization, and Multithreading. *Journal of Computational Chemistry* 2009, 31 (2), 455–461. DOI:10.1002/jcc.21334.
- [16]. Jumper, J.; Evans, R.; Pritzel, A.; Green, T.; Figurnov, M.; Ronneberger, O.; Tunyasuvunakool, K.; Bates, R.; Žídek, A.; Potapenko, A.; Bridgland, A.; Meyer, C.; Kohl, S. a. A.; Ballard, A. J.; Cowie, A.; Romera-Paredes, B.; Nikolov, S.; Jain, R.; Adler, J.; Back, T.; Petersen, S.; Reiman, D.; Clancy, E.; Zielinski, M.; Steinegger, M.; Pacholska, M.; Berghammer, T.; Bodenstein, S.; Silver, D.; Vinyals, O.; W, A., Senior; Kavukcuoglu, K.; Kohli, P.; Hassabis, D. Highly accurate protein structure prediction with AlphaFold. Nature 2021, 596 (7873), 583–589. DOI:10.1038/s41586-021-03819-2.
- [17]. Varadi, M.; Anyango, S.; Deshpande, M.; Nair, S.; Natassia, C.; Yordanova, G.; Yuan, D.; Stroe, O.; Wood, G.; Laydon, A.; Židek, A.; Green, T.; Tunyasuvunakool, K.; Petersen, S.; Jumper, J.; Clancy, E.; Green, R.; Vora, A.; Lutfi, M.; Figurnov, M.; Cowie, A.; Hobbs, N.; Kohli, P.; Kleywegt, G.; Birney, E.; Hassabis, D.; Velankar, S. AlphaFold Protein Structure Database: massively expanding the structural coverage of protein-sequence space with high-accuracy models. *Nucleic Acids Research* 2021, 50 (D1), D439–D444. DOI:10.1093/nar/gkab1061.
- [18]. Schrödinger, L.; DeLano, W. PyMOL.**2020**, Retrieved from http://www.pymol.org/pymol.
- [19]. Sanner MF. Python: a programming language for software integration and development. *J Mol Graph Model* **1999**, *17*(1), 57-61.
- [20]. Adasme, M. F.; Linnemann, K. L.; Bolz, S. N.; Kaiser, F.; Salentin, S.; Haupt, V. J.; Schroeder, M. PLIP 2021: Expanding the Scope of the Protein–Ligand Interaction Profiler to DNA and RNA. *Nucleic Acids Research* 2021, 49 (W1). DOI:10.1093/nar/gkab294.